Peak current control of grid-feeding inverter with low voltage ride-through capability

Sepannur Bandri, Zuriman Anthony, Erhaneli, Fauzan Ismail
Department of Electrical Engineering, Faculty of Engineering, Padang Institut of Technology, Padang, Indonesia

Article Info

ABSTRACT

The grid-feeding inverter is the most popular choice for implementing a distributed generator (DG) in a photovoltaic (PV) system. Its role is to deliver active power with zero reactive power while connected to the grid. In most cases, the inverter is disconnected as soon as voltage sag disturbances occur, an operation that is known as an islanding mode. Recently, grid code regulations have been upgraded, allowing the inverter to remain connected to the grid and inject a certain amount of reactive power during voltage sags, provided that it meets grid code requirements. However, this can result in an increase in current injection by the inverter, which may cause overcurrent and damage the inverter if it exceeds the capability of the inverter. To control peak current during voltage sag disturbances, a proposed grid-feeding inverter attempts to detect voltage sag and calculate proportional injected active and reactive power. Once the disturbance has disappeared from the system, the inverters can be restored to normal operation. Prototype experiments have validated the ability of this system to control peak current during voltage sag while protecting the inverters.

Corresponding Author:

Sepannur Bandri
Department of Electrical Engineering, Faculty of Engineering, Padang Institute of Technology
Jl. Gajah Mada Jl. Kandis Raya, Kp. Olo, Kec. Nanggalo, Padang, West Sumatera 25173, Indonesia
Email: sepannurb@yahoo.com

1. INTRODUCTION

Currently, distributed generators (DGs) are more prevalent in supporting the primary grid functionality, ensuring the availability of electricity for daily activities [1]-[5]. Thus, if an inverter system plays a significant role in ensuring the reliability and safety of a DG, it should be designed with intelligent functionality. It is essential that the capability to inject power into the network complies with the requirements of the grid code and has self-protection capabilities owing to the limitations of power injection from the inverter during faults [6]-[12]. Several conditions may cause it to be disconnected or to remain connected.

Disconnecting the DG from the grid during faults reduces power consumption and makes the system unstable. The system should provide power to the grid during faults using the fault-tolerance capabilities of the system [13]. IEEE has a policy to implement low-voltage ride-through (LVRT) for inverter systems to maintain voltage stability. Inverters can provide reactive power to a grid when the voltage is less than 0.9 of the rated voltage [14], [15]. Other methods limit the current during voltage-stability operations [16]-[18]. The LVRT strategy enhances system safety by injecting reactive current, reducing active power generation, addressing inductive line impedance for optimal performance, and employing direct current (DC)-link voltage control to maintain stability during grid voltage drops [19]. The circuit of a DC chopper and the controller limits an active current can improved the performance [20], [21]. It can maximize power delivery based on the maximum rated current [22].

Several current-limiting strategies have been proposed. First, the instantaneous saturation limits show how to consider the limit inductor current reference, where the current threshold is twice the peak current of the inverter [18], [23]. Second, the latch limit strategy that employs reference of inductor current and the natural reference frame (NRF) in its application [18], [24]. Third, the magnitude current limits were applied to the current limiting factor (CLF). This prevents the current reference from surpassing its limit when a fault occurs [18]. Fourth, a power state equation with an improved Lyapunov controller was applied to the current-limiting strategy [25]. The technique has the capability to restrict the fault current to a magnitude that is 1.5 times greater than the specified current. Fifth, the sequence-based control strategy considers positive and negative sequence components under asymmetrical faults [26]. Strengths and weaknesses were observed in all the aforementioned techniques. However, the complexity of these methods must also be considered.

The proposed inverter has outer and inner loops for power and current control, respectively. Both loops use dual proportional integral (PI) controllers in a cascaded connection. The power loop is regulated by the outer loop, which is determined by inverter capacity. The output of the power loop affects the inner loop, which regulates a suitable current. To prevent overcurrent damage, the inverter has a peak-current limit. The injected current amplitude was calculated using the dq-frame of the feedback current, which should not exceed the maximum current level. The main achievements of this study are summarized as follows: i) the grid-feeding inverter with LVRT capability was connected to the primary grid during the voltage sag and ii) a peak-current control technique limits the overcurrent and protects the inverter during the transitions.

The remainder of this study is structured as follows. Section 2 thoroughly investigates the proposed system, encompassing both its setup and regulations. Section 3 presents an evaluation of the prototype experiment along with the corresponding discoveries and verification of the proposed method. Finally, conclusions are presented in section 4.

2. METHOD

This study presents a grid-feeding inverter system, as depicted in Figures 1 and 2. The proposed system that has been suggested ensures that electricity is provided to the main power network in compliance with the specifications outlined in the grid code. The use of control techniques to limit the current under LVRT operation to overcome grid voltage sags demonstrates the impact of combining power control and current control. Consequently, the proportional injection of active and reactive powers maintains the peak of the injected current into the primary grid.

2.1. Proposed grid-feeding inverter

The grid-feeding inverter is a classified converter operated in the grid-connected mode, which is necessary for the reference voltage amplitude and frequency from another source to set an output [27]. A high-impedance grid current source connected parallel to the grid represents the grid-feeding inverter, as shown in Figure 1(a). Where the delivered active and reactive powers are denoted as P^* and Q^*, respectively. By implementing an inner current loop, the system can perfectly generate and synchronize the AC output voltage. Generally, this converter operates and connects to the grid; however, it can be connected in parallel with a grid-forming or grid-supporting inverter during the islanding mode.

Figure 1(b) illustrates the single-line circuit of the proposed grid-feeding inverter. The system uses an inductor and capacitor LC configuration to filter the output of the inverters, where the inverter voltage becomes the filtered inverter voltage V_i. The filter capacitor, filter inductance, and parasitic resistance are denoted as C_f, L_f, and R_c, respectively. Similarly, the grid impedance is composed of the grid inductance and grid resistance. These are denoted by L_g and R_g, respectively. Furthermore, the interconnected point between the inverter and grid system, namely the point of connection denoted with V_{pcc}, is also shown in the diagram.

This inverter operates in a grid-connected mode, providing active power to the grid, and uses a synchronous reference frame phase-lock loop (SRF-PLL). This method ensures that the voltage amplitude and frequency of the inverter are matched to the grid voltage and generates an aligned phase angle θ between V_i and V_g. An inverter with a power and current controller was employed to achieve the grid code standard, as illustrated in Figure 1(c).

The dq-reference frame is used to convert $I_{L_{abc}}$ and $V_{i_{abc}}$ to I_{dq} and V_{dq}, respectively. These variables become feedback signals to the power and current controllers. Therefore, the generated instantaneous powers of active and reactive can be expressed as (1)-(4):

$$P = \frac{\omega_c}{s+\omega_c}p \tag{1}$$

$$Q = \frac{\omega_c}{s+\omega_c}q \tag{2}$$

$$p = 1.5\big(V_d I_d + V_q I_q\big) \tag{3}$$

$$q = 1.5\big(V_q I_d - V_d I_q\big) \tag{4}$$

where the filtered active and reactive powers (P, Q) can be derived using (1) and (2), and both instantaneous active power and instantaneous reactive power are denoted by p in (3) and q in (4), respectively.
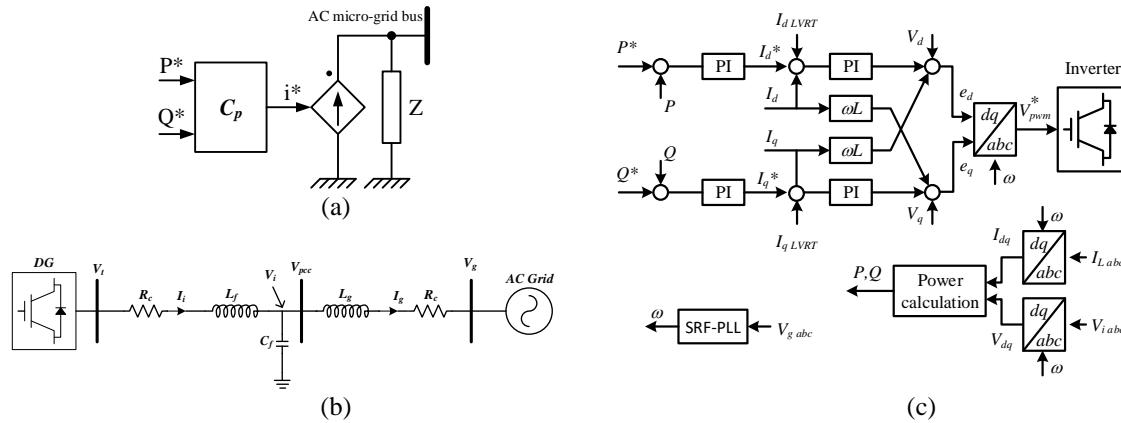

Figure 1. Model of a grid-feeding inverter; (a) circuit, (b) single line diagram, and (c) model of controller

Both PI controllers are utilized to generate the reference of active and reactive currents denoted as I_{dq}^*, as well as the reference of active and reactive voltages V_{dq}^*. Furthermore, the dq-frame converts the V_{dq}^*, becomes the magnitude voltage reference of the PWM that can be denoted as $\big(V_{pwm}^*\big)$. Hence, the dq-frame of the voltages error are writen as (5) and (6):

$$e_d = V_d + \big(K_{pi} + K_{ii}/s\big)\Big(\big((P^* - P)\big(K_{pp} + K_{ip}/s\big)\big) - I_d - I_{d_{LVRT}}\Big) - I_q \omega L_f \tag{5}$$

$$e_q = V_q + \big(K_{pi} + K_{ii}/s\big)\Big(\big((Q^* - Q)\big(K_{pp} + K_{ip}/s\big)\big) - I_d - I_{d_{LVRT}}\Big) - I_q \omega L_f \tag{6}$$

and V_{pwm}^* can be written in matrix form.

$$V_{pwm}^* = \begin{bmatrix} V_a^{ref} \\ V_b^{ref} \\ V_c^{ref} \end{bmatrix} = \begin{bmatrix} \sin(\omega t) & \cos(\omega t) & 1 \\ \sin(-120^o + \omega t) & \cos(-120^o + \omega t) & 1 \\ \sin(120^o + \omega t) & \cos(120^o + \omega t) & 1 \end{bmatrix} \begin{bmatrix} e_d \\ e_q \\ e_o \end{bmatrix} \tag{7}$$

2.2. Grid code requirement

Conventionally, a DG must be disconnected from the grid when experiencing a voltage sag and was only able to resynchronize once the fault had been rectified [28]-[30]. However, the use of advanced microgrids with smart inverters ensures a reliable power supply by actively sustaining active power delivery and providing reactive power support during voltage sags [31]. Prevention of potential instability can be achieved using an inverter system [32]. Consequently, under challenging circumstances, the microgrid ensures a smooth and reliable operation.

Figure 2(a) shows the rule of the inverter when detects grid voltage drops. The inverter disconnects from the grid below a certain threshold, but within acceptable voltage reduction limits, it remains connected using the LVRT strategy to adjust the reactive power delivery, as shown in Figure 2(b). Consequently, the inverter must increase k% of injected current if the grid voltage drops about 1% less than 0.9 V_N.
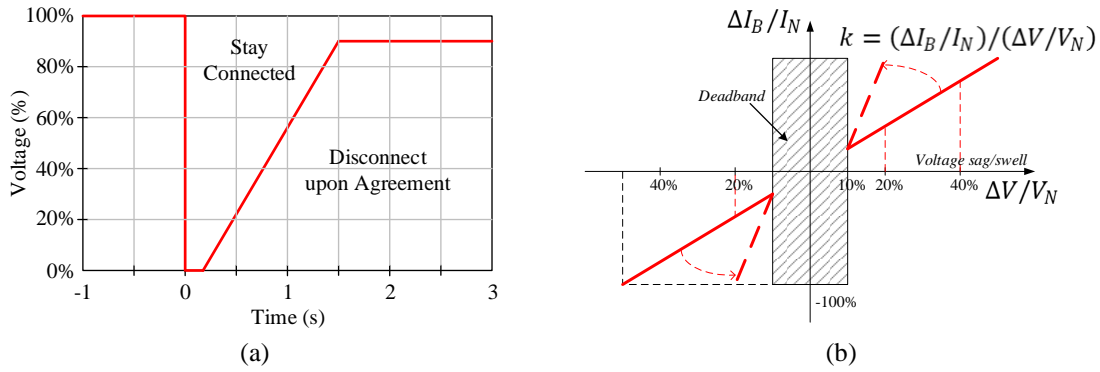
Figure 2. Requirement for grid code; (a) capability for LVRT and (b) capability to support reactive power

$$I_{q_{ref}} = \begin{cases} 0, & V_g > 0.9V_N \\ \left(-k.\frac{V_g}{V_N} + k\right) I_N, & 0.9V_N \geq V_g > 0.5V_N \\ I_N, & V_g \leq 0.5V_N \end{cases}$$

(8)

In (8) determines the requirement of the injected reactive power to ensure the stability and reliability of the inverter under the voltage sag condition. In which, the nominal voltage of grid (V_N) and converter rated current (I_N) play significant roles. The extent of the voltage sag (ΔV) and the increase in reactive current (ΔI_B) following a fault are also crucial factors. It is worth mentioning that the German grid code [32] mandates a minimum value of 2 p.u for a constant k to ensure stability and reliability in the system.

2.3. Peak current control under voltage sag disturbance

This method limits inverter current injection during a grid voltage sag, allowing the inverter to remain connected to the injected power. It involves measuring real-time grid voltage to calculate a sag signal, which then determines the active current reference I_d^* and reactive current reference I_q^*. Where the proposed LVRT strategy ensures an optimal reactive power injection (RPI) during voltage sags.

2.3.1. Sag detection

Figure 3 provides a visual representation of the conventional synchronous rotating reference frame (CSRRF), which is used as a voltage detection technique [33]. The essence of this technique lies in its ability to identify voltage sag using the abc-dq transformation. This transformation enables the calculation of DC quantities (V_d, V_q) that are directly proportional to AC grid voltage (V_a, V_b, V_c). The relationship between DC and AC quantities can be expressed as (9):

$$\begin{bmatrix} V_d \\ V_q \end{bmatrix} = \frac{2}{3} \begin{bmatrix} \cos \omega t & -\sin \omega t \\ \sin \omega t & \cos \omega t \end{bmatrix} \begin{bmatrix} 1 & -1/2 & -1/2 \\ 0 & \sqrt{3}/2 & -\sqrt{3}/2 \end{bmatrix} \begin{bmatrix} V_a \\ V_b \\ V_c \end{bmatrix}$$

(9)

According to the information provided in Figure 3, the sag signal is produced through the generation of a filtered V_{dq}, which is determined by the square root of the sum of the squared V_d and V_q values. This resultant signal was then subjected to comparison with a DC reference in the comparator, specifically set at 0.9 per unit (pu). It is important to note that the variation in V_{dq} is directly associated with the measured grid voltage, and to ensure the removal of the 100 Hz component or 2ω, a low-pass filter (LPF) is employed.
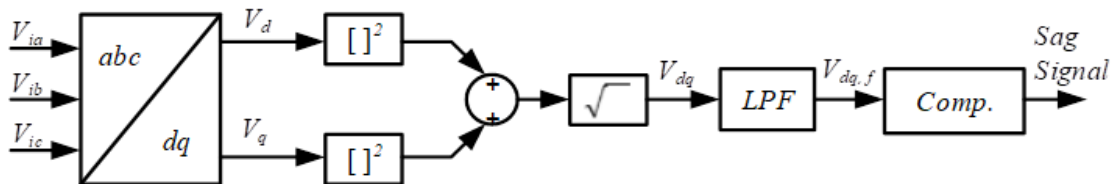

Figure 3. CSRRF-based voltage sag detection

2.3.2. LVRT operation mode

The smart grid-feeding inverter must fulfil grid code requirements by injecting active and reactive power [34], necessitating a design to limit the current during abnormal operations.

$$
\begin{cases}
I_q = I_N, & 0 \le v_g < \left(1 - \frac{1}{k}\right) p.u. \\
I_q = k\left(1 - v_g\right)I_N, & \left(1 - \frac{1}{k}\right) p.u. \le v_g < 0.9\, p.u.
\end{cases}
\tag{10}
$$

RPI control is activated when there is a drop in the grid voltage to ensure compliance with the specified amount of reactive current outlined in the German grid code, as shown in Figure 2(a) [35]. An injected current based on real-time grid voltage levels is required to maintain system stability under fault ride-through. This involves assessing the connection between the initial reactive current (I_{q0}) and real-time voltage levels (v_g) during a voltage sag, as (11):

$$
= \frac{(I_q - I_{q0})/I_N}{(1 - v_g)}, \text{ when } I_q < I_N
\tag{11}
$$

where $k \ge 2\, p.u.$

$$
I_{g\,max} = \sqrt{I_d^2 + I_q^2} \le I_{max}
\tag{12}
$$

The key current parameters in the inverter system, such as active current (I_d), injected current amplitude ($I_{g\,max}$), and maximum allowable current (I_{max}). This emphasizes the significance of preventing overloading and ensuring the inverter operates within specified limits, with proposed RPI strategies outlined in (10) and (12). Potential risks associated with RPI strategies and overcurrent loading in LVRT modes have led to the introduction of a new control strategy called *Const.-Igmax*. This strategy aims to prevent unintended inverter shutdowns by maintaining a consistently subordinate peak current injection from the grid, always below the inverter's current threshold (I_{max}). Specific conditions, involving the relationship between maximum grid current ($I_{g\,max}$), nominal current (I_N), and the control strategy's success, are outlined, with a specified range of grid voltage disruptions where (10) for current calculation in the dq-frame is valid when the grid voltage drops disruption in the range of $\left(1 - (1/k)\right)p.u \le V_g < 0.9\, p.u.$

$$
\begin{cases}
I_d = \sqrt{n^2 - k^2\left(1 - v_g\right)^2}\, I_N \\
I_q = k\left(1 - v_g\right)I_N
\end{cases}
\tag{13}
$$

As mentioned in (12), when the grid voltage drops below $\left(1 - (1/k)\right)p.u$, it is necessary to adjust the current in the dq-frame.

$$
\begin{cases}
I_d = \sqrt{n^2 - 1}\, I_N \\
I_q = I_N
\end{cases}
\tag{14}
$$

The maximum value of n that determines the inverter current protection, can be calculated using the equation $(I_{max}/I_N)p.u.$ To ensure that the inverter remains stable during RPI, it is recommended to design with a margin of 2 per unit ($I_{max} = 2I_N$), resulting in a maximum value of n equal to 2 per unit. By setting n equal to (I_{max}/I_N), the inverter's riding-through operation will not amplify the injected grid current. Additionally, during the LVRT mode, the active power is reduced based on (13) and (15) to facilitate the injection of sufficient reactive power.

$$
P = \frac{3}{2}V_{gm}I_d
\tag{15}
$$

The amplitude of the grid voltage is denoted by V_{gm}.

3.   RESULTS AND DISCUSSION

The experimental setup of the prototype system is shown in Figure 4. The proposed inverter functioned to feed power to the grid seamlessly. Its sophisticated design helps maintain high-quality power transmission and system performance at its optimal levels while meeting the specific operational requirements of the grid-feeding inverter. The list of the experimental parameters is presented in Table 1.
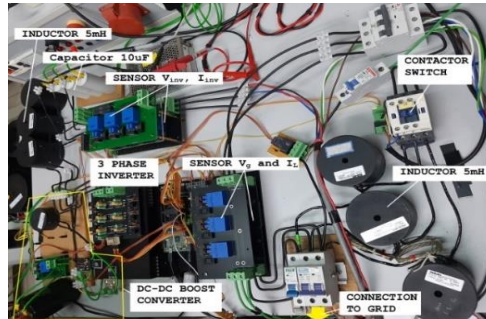

Figure 4. Experimental configuration

Table 1. Inverter system parmeters

Name of parameter	Value
Rated voltage of the inverter	115 V
Inductance	5 mH
Capacitance	10 uF
Switching frequency (f_{sw})	20 kHz
Rate frequency (f)	50 Hz
Transformer ratio	115:415

Validation tests were conducted on a grid-feeding inverter in both grid-connected and voltage-sag disturbance scenarios. Figure 5 shows a snapshot of the inverter's performance, with 1.4% of the voltage harmonics in Figure 5(a) and 4.3% of the current harmonics in Figure 5(b). In this experiment, two scenarios were used to validate the performance. Figure 6(a) shows the results for constant active power control and injected reactive power. Under normal grid conditions, the inverter injected 0.270 p.u of active power (P) and 0 p.u of reactive power (Q), maintaining V_{inv} at 65.77 V and I_{inv} at 1.515 A. During a disturbance in which the grid voltage drops to less than 20% of the normal value, the inverter aims to inject 0.263 p.u (263 VAr) of reactive power while maintaining the active power constant at 0.270 p.u. (270 W). The phase angle shift between the voltage and current indicates the injected reactive power, and the experiment showed a current lagging voltage of approximately 60°, resulting in an increased current to 3.044 A and an unpredicted fluctuating current during the initial voltage sag.
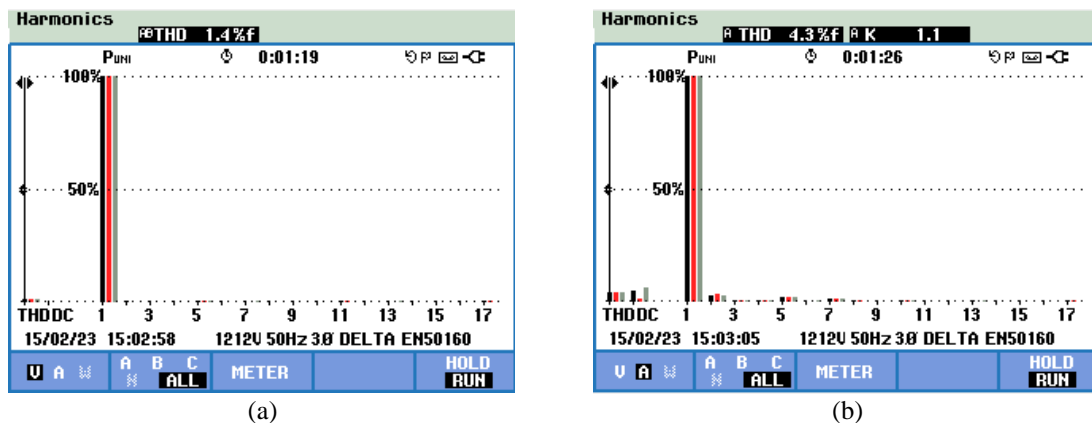

Figure 5. Grid feeding inverter performance under grid-connected mode; (a) voltage harmonics and (b) current harmonics

Figure 6(b) presents the outcomes of our proposed method and scenario, wherein we implemented peak-current control within our experimental setup. Regardless of whether the grid operates under normal conditions or experiences a voltage sag disturbance, the inverter adeptly maintains the peak current. However, under voltage sag conditions, the inverter current exhibits a phase lag of more than 60° relative to the voltage. This lag results in discernible effects, as the active power output decreases from 0.302 p.u. (equivalent to 302 watts) to 0.135 p.u. (135 watts), while the reactive power output increases from 0 p.u (0 VAr) to 0.239 p.u. (239 VAr). Ultimately, these findings confirm the effectiveness of the proposed control method in limiting the inverter current that effectively safeguards the inverter against grid voltage-drop events.

(a)   (b)
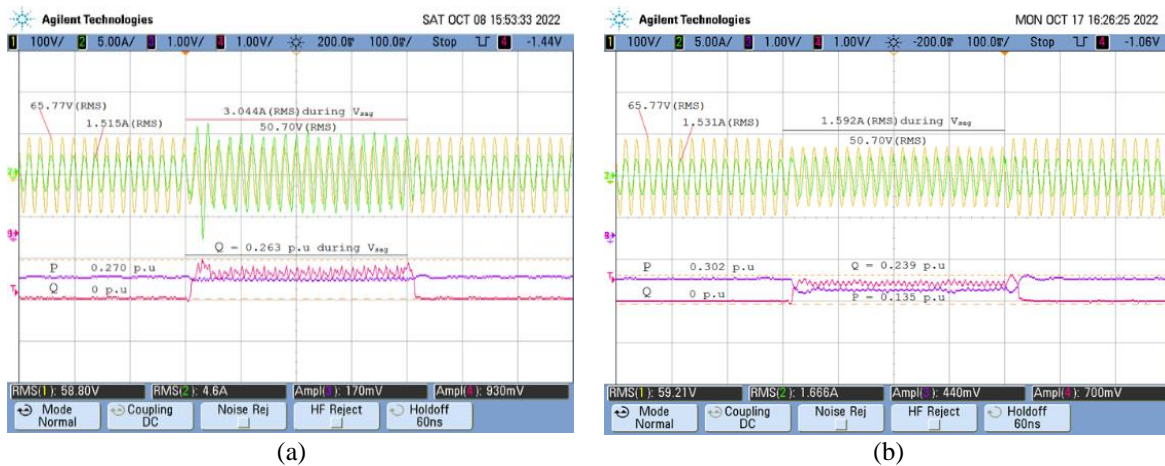
Figure 6. Grid-feeding inverter test when the grid voltage drop (k=2 and n=0.5); (a) constant active power and (b) peak current control

4. CONCLUSION

This work presents the designing inverter feeds power to grid to be operated for normal also abnormal grid condition. Under normal grid-connected mode, current harmonic and voltage harmonic of the inverter shows value 1.4% and 4.3%, which validated by Fluke 435-II power analyzer, respectively. Particularly during grid voltage drops, voltage sag detection technique based on CSRRF is ensured capable to detects fastly. Meanwhile, the system injects a number of reactive power and remains connected to the primary grid. Conventional constant active power control shows spikes in current on the transition time of the voltage sag, however, active power remains constant. Due to this reason, the peak current control technique is implemented to maintain a constant peak current, although the inverter is disturbed by voltage sag. The inverters prototype involved peak current control under LVRT mode is validated with experimental test. It means the inverter injected reactive power by reducing active power delivery. Therefore, the proposed technique provides satisfactory performance to avoid over-current conditions during voltage sag.

REFERENCES

[1] H. Hui, Y. Chen, S. Yang, H. Zhang, and T. Jiang, "Coordination control of distributed generators and load resources for frequency restoration in isolated urban microgrids," *Applied Energy*, vol. 327, p. 120116, 2022, doi: 10.1016/j.apenergy.2022.120116.
[2] M. Rajeev and V. Agarwal, "Low Voltage Ride-Through Capability of a Novel Grid Connected Inverter Suitable for Transformer-Less Solar PV-Grid Interface," *IEEE Transactions on Industry Applications*, vol. 56, no. 3, pp. 2799–2806, 2020, doi: 10.1109/TIA.2020.2979134.
[3] M. A. G. Lopez, J. L. G. De Vicuna, J. Miret, M. Castilla, and R. Guzman, "Control Strategy for Grid-Connected Three-Phase Inverters during Voltage Sags to Meet Grid Codes and to Maximize Power Delivery Capability," *IEEE Transactions on Power Electronics*, vol. 33, no. 11, pp. 9360–9374, 2018, doi: 10.1109/TPEL.2018.2792478.
[4] M. Yu, W. Huang, N. Tai, X. Zheng, P. Wu, and W. Chen, "Transient stability mechanism of grid-connected inverter-interfaced distributed generators using droop control strategy," *Applied Energy*, vol. 210, pp. 737–747, 2018, doi: 10.1016/j.apenergy.2017.08.104.
[5] Y. Yang, K. Zhou, and F. Blaabjerg, "Current Harmonics From Single-Phase Grid-Connected Inverters—Examination and Suppression," in *IEEE Journal of Emerging and Selected Topics in Power Electronics*, vol. 4, no. 1, pp. 221–233, Mar. 2016, doi: 10.1109/JESTPE.2015.2504845.

[6] M. Nasiri and R. Mohammadi, "Peak Current Limitation for Grid Side Inverter by Limited Active Power in PMSG-Based Wind Turbines During Different Grid Faults," *IEEE Transactions on Sustainable Energy*, vol. 8, no. 1, pp. 3–12, 2017, doi: 10.1109/TSTE.2016.2578042.

[7] Y. Yang, F. Blaabjerg, and H. Wang, "Low-voltage ride-through of single-phase transformerless photovoltaic inverters," *IEEE Transactions on Industry Applications*, vol. 50, no. 3, pp. 1942–1952, 2014, doi: 10.1109/TIA.2013.2282966.

[8] R. L. Lima, J. P. Bonaldo, J. C. M. Vieira, and R. M. Monaro, "A Graphical Method to Assess the Technical Feasibility of Intentional Islanding of Distributed Synchronous Generators," *IEEE Transactions on Power Delivery*, vol. 38, no. 1, pp. 742–745, 2023, doi: 10.1109/TPWRD.2022.3220087.

[9] A. Mojallal and S. Lotfifard, "Enhancement of Grid Connected PV Arrays Fault Ride Through and Post Fault Recovery Performance," *IEEE Transactions on Smart Grid,* vol. 10, no. 1, pp. 546–555, 2019, doi: 10.1109/TSG.2017.2748023.

[10] G. P. V Inverters and E. Current, "Control Strategy for Three-Phase Limitation Under Unbalanced Faults," *IEEE Transactions on Industrial Electronics*, vol. 64, no. 11, pp. 8908–8918, 2017.

[11] M. E. El-Hawary, "Power engineering letters," *IEEE Power Engineering Review*, vol. 22, no. 10, p. 43, 2002, doi: 10.1109/MPER.2002.1005652.

[12] C. Nithya and J. P. Roselyn, "Multimode Inverter Control Strategy for LVRT and HVRT Capability Enhancement in Grid Connected Solar PV System," *IEEE Access*, vol. 10, pp. 54899–54911, 2022, doi: 10.1109/ACCESS.2022.3175872.

[13] D. M. Vilathgamuwa, P. C. Loh, and Y. Li, "Protection of microgrids during utility voltage sags," *IEEE Transactions on Industrial Electronics*, vol. 53, no. 5, pp. 1427–1436, 2006, doi: 10.1109/TIE.2006.882006.

[14] H. D. Tafti, A. I. Maswood, G. Konstantinou, J. Pou, and P. Acuna, "Active / reactive power control of photovoltaic grid-tied inverters with peak current limitation and zero active power oscillation during unbalanced voltage sags," *IET Power Electronics*, vol. 11, no. 6, pp. 1066–1073, 2018, doi: 10.1049/iet-pel.2017.0210.

[15] J. Miret, A. Camacho, M. Castilla, L. G. de Vicuña, and J. Matas, "Control Scheme With Voltage Support Capability for Distributed Generation Inverters Under Voltage Sags," in *IEEE Transactions on Power Electronics*, vol. 28, no. 11, pp. 5252-5262, Nov. 2013, doi: 10.1109/TPEL.2013.2246190.

[16] T. Zheng, L. Chen, Y. Guo, and S. Mei, "Flexible unbalanced control with peak current limitation for virtual synchronous generator under voltage sags," *Journal of Modern Power Systems and Clean Energy*, vol. 6, no. 1, pp. 61–72, 2018, doi: 10.1007/s40565-017-0295-y.

[17] H. R. Baghaee, M. Mirsalim, G. B. Gharehpetian, and H. A. Talebi, "A new current limiting strategy and fault model to improve fault ride-through capability of inverter interfaced DERs in autonomous microgrids," *Sustainable Energy Technologies and Assessments*, vol. 24, pp. 71–81, 2017, doi: 10.1016/j.seta.2017.02.004.

[18] I. Sadeghkhani, M. E. H. Golshan, J. M. Guerrero and A. Mehrizi-Sani, "A Current Limiting Strategy to Improve Fault Ride-Through of Inverter Interfaced Autonomous Microgrids," in *IEEE Transactions on Smart Grid*, vol. 8, no. 5, pp. 2138-2148, Sep. 2017, doi: 10.1109/TSG.2016.2517201.

[19] Y. He, M. Wang, Y. Jia, J. Zhao, and Z. Xu, "Low-voltage ride-through control for photovoltaic generation in the low-voltage distribution network," *IET Renewable Power Generation*, vol. 14, no. 14, pp. 2727–2737, Oct. 2020, doi: 10.1049/iet-rpg.2019.1101.

[20] R. Ntare, N. H. Abbasy, and K. H. M. Youssef, "Low Voltage Ride through Control Capability of a Large Grid Connected PV System Combining DC Chopper and Current Limiting Techniques," *Journal of Power and Energy Engineering*, vol. 07, no. 01, pp. 62–79, 2019, doi: 10.4236/jpee.2019.71004.

[21] Y. Geng, K. E. Yang, Z. O. U. Lai, P. Zheng, H. Liu, and R. Deng, "A Novel Low Voltage Ride Through Control Method for Current Source Grid-Connected Photovoltaic Inverters," *IEEE Access*, vol. 7, pp. 51735–51748, 2019, doi: 10.1109/ACCESS.2019.2911477.

[22] J. L. Sosa, M. Castilla, J. Miret, J. Matas, and Y. A. Al-Turki, "Control Strategy to Maximize the Power Capability of PV Three-Phase Inverters During Voltage Sags," in *IEEE Transactions on Power Electronics*, vol. 31, no. 4, pp. 3314–3323, Apr. 2016, doi: 10.1109/TPEL.2015.2451674.

[23] C. A. Plet, M. Graovac, T. C. Green, and R. Iravani, "Fault response of grid-connected inverter dominated networks," in *IEEE PES General Meeting, PES 2010*, 2010, pp. 1–8, doi: 10.1109/PES.2010.5589981.

[24] N. Bottrell and T. C. Green, "Comparison of current-limiting strategies during fault ride-through of inverters to prevent latch-up and wind-up," *IEEE Transactions on Power Electronics*, vol. 29, no. 7, pp. 3786–3797, 2014, doi: 10.1109/TPEL.2013.2279162.

[25] T. Li, Y. Li, X. Chen, S. Li, and W. Zhang, "Research on AC Microgrid with Current-Limiting Ability Using Power-State Equation and Improved Lyapunov-Function Method," *IEEE Journal of Emerging and Selected Topics in Power Electronics*, vol. 9, no. 6, pp. 7306–7319, 2021, doi: 10.1109/JESTPE.2020.3013230.

[26] B. Mahamedi, M. Eskandari, J. E. Fletcher, and J. Zhu, "Sequence-Based Control Strategy with Current Limiting for the Fault Ride-Through of Inverter-Interfaced Distributed Generators," *IEEE Transactions on Sustainable Energy*, vol. 11, no. 1, pp. 165–174, 2020, doi: 10.1109/TSTE.2018.2887149.

[27] J. Rocabert, A. Luna, F. Blaabjerg and P. Rodríguez, "Control of Power Converters in AC Microgrids," in *IEEE Transactions on Power Electronics*, vol. 27, no. 11, pp. 4734–4749, Nov. 2012, doi: 10.1109/TPEL.2012.2199334.

[28] "IEEE Standard for Interconnecting Distributed Resources with Electric Power Systems," in *IEEE Std 1547-2003* , pp. 1-28, Jul. 2003, doi: 10.1109/IEEESTD.2003.94285.

[29] M. R. Islam and H. A. Gabbar, "Study of Micro Grid Safety & Protection Strategies with Control System Infrastructures," *Smart Grid and Renewable Energy*, vol. 03, no. 01, pp. 1–9, 2012, doi: 10.4236/sgre.2012.31001.

[30] F. Wang, J. L. Duarte, and M. A. M. Hendrix, "Pliant active and reactive power control for grid-interactive converters under unbalanced voltage dips," in *IEEE Transactions on Power Electronics*, vol. 26, no. 5, pp. 1511–1521, May 2011, doi: 10.1109/TPEL.2010.2052289.

[31] F. Ismail, A. Effendi, and W. Witrionanda, "Power Injection on Single Phase Grid System," *Elkha*, vol. 11, no. 1, p. 47, 2019, doi: 10.26418/elkha.v11i1.30932.

[32] X. Zhao, J. M. Guerrero, M. Savaghebi, J. C. Vasquez, X. Wu, and K. Sun, "Low-voltage ride-through operation of power converters in grid-interactive microgrids by using negative-sequence droop control," *IEEE Transactions on Power Electronics*, vol. 32, no. 4, pp. 3128–3142, 2017, doi: 10.1109/TPEL.2016.2570204.

[33] Y. Kumsuwan and Y. Sillapawicharn, "A fast synchronously rotating reference frame-based voltage sag detection under practical grid voltages for voltage sag compensation systems," *6th IET International Conference on Power Electronics, Machines and Drives (PEMD 2012)*, Bristol, 2012, pp. 1–5, doi: 10.1049/cp.2012.0348.

[34] Y. Yang, H. Wang, and F. Blaabjerg, "Reactive Power Injection Strategies for Single-Phase Photovoltaic Systems Considering Grid Requirements," in *IEEE Transactions on Industry Applications*, vol. 50, no. 6, pp. 4065–4076, Nov.-Dec. 2014, doi: 10.1109/TIA.2014.2346692.

[35] Y. Bae, T. K. Vu, and R. Y. Kim, "Implemental control strategy for grid stabilization of grid-connected PV system based on German grid code in symmetrical low-to-medium voltage network," *IEEE Transactions on Energy Conversion*, vol. 28, no. 3, pp. 619–631, 2013, doi: 10.1109/TEC.2013.2263885.

BIOGRAPHIES OF AUTHORS

Sepannur Bandri received the B.Eng. degree from the University of Bung Hatta, Padang, Indonesia, the M.Eng. degree from the Bandung Institute of Technology, and Ph.D. degree from Padang State University, Padang, Indonesia in 2020. He is currently a Lecturer at Padang Institute of Technology. His research interests include energy conversion, electrical machines, and renewable energy. He can be contacted at email: sepannurb@yahoo.com.

Zuriman Anthony is a man who is actively involved in many research activities. This man is active in the electrical engineering department of the Institute of Technology Padang (Institut Teknologi Padang (ITP)), which also lectures on electrical machines. His research activity includes energy conversion, electrical machines, and power system analysis. He received the Bachelor of Engineering in Electric Power System from the Institute of Technology Padang, Padang, West Sumatera in 1996, and the Master of Engineering in electrical power engineering from Gadjah Mada University, Yogyakarta in 2002. He can be contacted at email: antoslah@gmail.com.

Erhaneli is a woman who actively participates in research group activities. Her interest in her research in the field of electrical machines and the distribution of the electrical network. She is active in the Department of Electrical Engineering of the Institute of Technology Padang, and also teaches power energy conversion and electrical power distribution. She can be contacted at email: erhanelimarzuki@gmail.com.

Fauzan Ismail received the B.Eng. degree from the University of Andalas, Padang, Indonesia, in 2004, and the M.Eng.Sc. degree in power electronics from the University of Malaya, Kuala Lumpur, Malaysia, in 2011. He is currently working toward the Ph.D. degree in power electronics at the University of Malaya, Malaysia. He joined the Department of Electrical Engineering, Padang Institute of Technology, as a Lecturer, in 2016. His research interests include power electronics and renewable energy. He can be contacted at email: fauzan.ismail@gmail.com.